Original Paper

Ex situ perfusion fixation for brain banking: a technical report

Andrew T. McKenzie[1,2,3,4], Emma Woodoff-Leith[1,2,3], Diana Dangoor[1,2,3], Alessandra Cervera[1,2,3], Hadley Walsh Ressler[1,2,3], Kristen Whitney[1,2,3], Kristen Dams-O'Connor[5,6], Zhuhao Wu[1,7,8], Elizabeth M. C. Hillman[9], Alan C. Seifert[10], John F. Crary[1,2,3]

[1] *Department of Neuroscience, Icahn School of Medicine at Mount Sinai, New York, New York, USA*

[2] *Friedman Brain Institute, Departments of Pathology, Neuroscience, and Artificial Intelligence & Human Health, Icahn School of Medicine at Mount Sinai, New York, New York, USA*

[3] *Neuropathology Brain Bank & Research Core and Ronald M. Loeb Center for Alzheimer's Disease, Icahn School of Medicine at Mount Sinai, New York, New York, USA*

[4] *Department of Psychiatry, Icahn School of Medicine at Mount Sinai, New York, New York, USA*

[5] *Department of Rehabilitation and Human Performance, Icahn School of Medicine at Mount Sinai, New York, New York, USA*

[6] *Department of Neurology, Icahn School of Medicine at Mount Sinai, New York, New York, USA*

[7] *Department of Cell, Developmental, and Regenerative Biology, Icahn School of Medicine at Mount Sinai, New York, New York, USA*

[8] *Black Family Stem Cell Institute, Icahn School of Medicine at Mount Sinai, New York, New York, USA*

[9] *Laboratory for Functional Optical Imaging, Departments of Biomedical Engineering and Radiology and the Mortimer B. Zuckerman Mind Brain Behavior Institute, Columbia University, New York, New York, USA*

[10] *Biomedical Engineering and Imaging Institute, Department of Diagnostic, Molecular and Interventional Radiology, and Graduate School of Biomedical Sciences, Icahn School of Medicine at Mount Sinai, New York, New York, USA*

Corresponding author:
John F. Crary · Department of Pathology · Icahn School of Medicine at Mount Sinai · Icahn Building 9th Floor, Room 20A · 1425 Madison Avenue · New York, NY 10029 · USA
john.crary@mountsinai.org

Abstract

Perfusion fixation is a well-established technique in animal research to improve preservation quality in the study of many tissues, including the brain. There is a growing interest in using perfusion to fix postmortem human brain tissue to achieve the highest fidelity preservation for downstream high-resolution morphomolecular brain mapping studies. Numerous practical barriers arise when applying perfusion fixation in brain banking settings, including the large mass of the organ, degradation of vascular integrity and patency prior to the start of the procedure, and differing investigator goals sometimes necessitating part of the brain to be frozen. As a result, there is a

critical need to establish a perfusion fixation procedure in brain banking that is flexible and scalable. This technical report describes our approach to developing an *ex situ* perfusion fixation protocol. We discuss the challenges encountered and lessons learned while implementing this procedure. Routine morphological staining and RNA *in situ* hybridization data show that the perfused brains have well-preserved tissue cytoarchitecture and intact biomolecular signal. However, it remains uncertain whether this procedure leads to improved histology quality compared to immersion fixation. Additionally, *ex vivo* magnetic resonance imaging (MRI) data suggest that the perfusion fixation protocol may introduce imaging artifacts in the form of air bubbles in the vasculature. We conclude with further research directions to investigate the use of perfusion fixation as a rigorous and reproducible alternative to immersion fixation for the preparation of postmortem human brains.

Introduction

A detailed examination of the brain in various settings, including educational, clinical, and research domains, is critically dependent upon the quality of brain preservation. Human tissue-based research, which plays a significant role in studying brain diseases, relies on the brain banking process to sufficiently preserve the postmortem brain. For example, in the study of brain disorders such as Alzheimer's disease, it is essential to have well-maintained histoarchitecture and biomolecular structure to reliably distinguish the features of brain donors with and without the disorder (Lucassen et al., 1997). The goal of the initial preservation procedure is to interrupt postmortem degradative processes in a way that prepares the brain for long-term storage, while minimizing damage resulting from the preservation process itself. With access to intact, well-preserved human brain tissue, investigators can conduct a diverse set of next-generation brain mapping studies, including high-resolution *ex vivo* neuroimaging (Pallebage-Gamarallage et al., 2018), connectomics studies using high-throughput serial section electron microscopy (Shapson-Coe et al., 2021), and volumetric 3D histologic imaging of the brain's cellular- and molecular-level organization (Patel et al., 2022).

All existing brain preservation procedures face trade-offs in the extent and type of tissue preservation achieved and the consequent degree of information loss. In non-human animal studies, perfusion fixation is widely considered to be the state of the art for achieving the highest-quality morphologic preservation of the whole brain (Bodian, 1936; Karlsson and Schultz, 1965; McFadden et al., 2019). In human tissue brain banking, immersion fixation is the most common preservation method employed. A key conundrum in immersion procedures is that the outer regions of the brain are liable to be over-fixed and the inner regions of the brain are liable to be under-fixed, both of which have the potential to limit optimal and consistent antigen preservation. While sectioning tissue prior to immersion may allow fixative to penetrate inner brain regions earlier, this technique can damage tissue morphology (Adickes et al., 1997). Perfusion fixation is a potential solution for this challenge and may more consistently preserve tissue morphology and antigenicity than immersion fixation. The perfusion technique may allow for a shorter fixation period, without requiring pre-sectioning, by penetrating inner brain regions more quickly. Perfusion fixation is also expected to limit tissue autolysis, a postmortem change that inevitably occurs in the inner brain regions before the immersion fixative can reach those areas (Beach et al., 1987; McFadden et al., 2019).

Perfusion can either be performed via an intrathoracic approach in the case of smaller animals or via an intracarotid approach in the case of larger animals such as pigs or elephants (Manger et al., 2009; Musigazi et al., 2018). The two classes of methods to perform perfusion fixation are *ex situ* methods, where the brain is extracted from the skull prior to perfusion, and *in situ* methods, where the brain remains inside the skull during perfusion (McFadden et al., 2019) (**Figure 1**). *In situ* approaches often involve cannulation of one or both
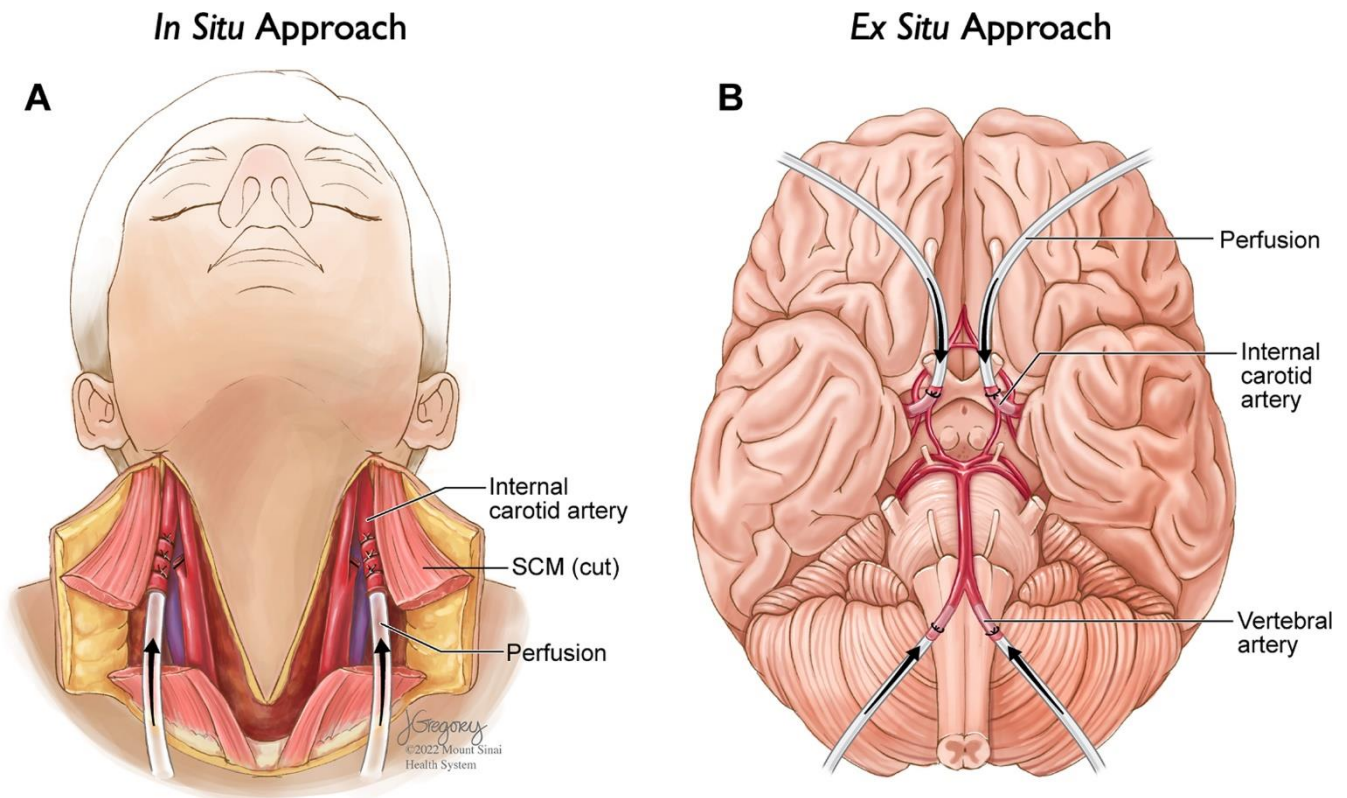
Figure 1. Two major approaches for performing perfusion fixation

Example approaches of human brain perfusion fixation using an *in situ* (brain inside of the skull); **A**) or *ex situ* (brain removed from the skull); **B**) approach. While only an *ex situ* perfusion protocol is described in this report, we include an illustration of the *in situ* method as well to demonstrate this alternative approach. Also, while the use of surgical sutures is an alternative approach that is illustrated here, in our protocol, hemostats are used to clamp cannulae in place. Arrows represent the direction of perfusate flow during perfusion. SCM = Sternocleidomastoid muscle. Illustrations by Jill K. Gregory, Certified Medical Illustrator, Fellow of the Association of Medical Illustrators.

carotid arteries, with or without also cannulating the vertebral arteries. *Ex situ* approaches often involve cannulation of the internal carotid arteries and the vertebrobasilar artery system.

The purpose of this technical report is to describe our use of perfusion fixation for human brain banking as a quality improvement project. We used an *ex situ* approach, which can be more easily integrated into the autopsy suite workflow and which is compatible with the anatomical donation of the brain alone, as opposed to a full-body donation. Our aim is to describe our experience in implementing this procedure to provide pertinent information for the research community.

There have been several previous descriptions of *ex situ* approaches to perfusion fixation in brain banking described in the literature (Adickes et al., 1997; Beach et al., 1987; de Oliveira et al., 2012;

Grinberg et al., 2008; Halliday et al., 1988; Insausti et al., 1995; Waldvogel et al., 2006; Welikovitch et al., 2018). We recognize that there are likely many other approaches. We also suspect that perfusion fixation methods in brain banking will likely evolve in the future as more researchers engage with the procedure.

Materials and Methods

Patient samples

All specimens were obtained and de-identified at the Icahn School of Medicine at Mount Sinai in accordance with its policies, regulations, and institutional review board recommendations. The use of the perfusion fixation protocol was developed as part of an ongoing quality improvement project in the Neuropathology Brain Bank & Research Core.

The goal of the project is to see whether it is possible to decrease fixation times and thereby mitigate antigenicity loss of formalin-sensitive antigens in intact brains. The specimens were a convenience sample of brains processed at the Neuropathology Brain Bank & Research Core, with no specific exclusion criteria.

Perfusion fixation methods

We used the same perfusion circuit setup throughout the development of the protocol, with or without an in-line pressure sensor. Details of the procedure, including the use of different reagents, were iterated upon over the course of the study. In our perfusion circuit, fluid in a beaker, which consists of either washout or fixative solution, is pumped through silicone tubing via a peristaltic pump with a variable pump drive speed, which mediates the flow rate (see **Table 1** for details of equipment used). Downstream of the pump, there is a pulse dampener that acts to prevent significant pulsations in fluid flow. The next component in the circuit is the pressure sensor, which connects to a digital pressure monitor. Finally, there is a Y connector that splits the circuit into two circuits, each of which connects to a catheter that can be used to cannulate one blood vessel. Following cannulation, the cannulae are clamped in place with hemostats in all cases. If it is preferred to perfuse through only one of the two catheters at a time, the perfusion tubing following the Y connector for the other catheter can be clamped with a hemostat to stop the flow through that component of the circuit. All perfusion procedures are performed at room temperature.

We performed this procedure on two types of specimens, termed either 'whole brain' or 'hemibrain'. The term hemibrain refers to one of the two cerebral hemispheres, which is obtained after a hemi-sectioning procedure designed to retain enough of the circle of Willis for adequate vascular access. Three hemi-brains (cases 1-3) and two whole brains (cases 4-5) were subjected to perfusion fixation. In case 1, the hindbrain was not removed prior

Table 1. Supplies and reagents

Equipment / Chemical	Supplier	Catalog Number
Masterflex Variable-Speed Digital Drive	Cole-Parmer	07528-10
Masterflex Pump Head Easy-Load II	Cole-Parmer	77200-60
Silicone Perfusion Tubing #14	Cole-Parmer	96400-16
Masterflex Y-Connector PE 1/8"	Cole-Parmer	30726-03
PendoTECH PressureMAT Monitor	Cole-Parmer	19406-60
PendoTECH Pressure Sensor	Cole-Parmer	19406-20
Pulse Dampener	Cole-Parmer	07596-20
Butterfly Catheter Infusion Set, 19 Gauge (19G)†	Harvard Apparatus	72-5960
Butterfly Catheter Infusion Set, 21 Gauge (21G)†	Harvard Apparatus	72-5963
Butterfly Catheter Infusion Set, 23 Gauge (23G)†	Harvard Apparatus	72-5964
Neutral Buffered Formalin	Fisher	245-685
Sodium Azide	Sigma Aldrich	CAS 26628-22-8
Glutaraldehyde	Fisher	G151-1
D-Mannitol	Fisher	AC423920050
Sodium Nitrite	Sigma-Aldrich	S2252

† Catheter bevels are filed to have blunt ends prior to use in perfusion.

to the perfusion procedure; however, in all other cases, the hindbrain was detached following transection through the upper midbrain to vascular access. Thus, whole brain specimens have both cerebral hemispheres, but some brainstem structures removed. There were a couple of differences in how perfusion fixation was performed for hemibrain and whole brain specimens. First, for hemibrains, a plastic container with muslin cloth was used to suspend the specimen without immersing it in fixative, allowing the perfusate to drain into the bottom of the container during the procedure. For whole brains, there was a focus on volumetric analysis with *ex vivo* neuroimaging. As a result, for the whole brain cases, the specimen was suspended in a formalin bath, because suspending the brain in fluid was expected to less shape deformation during the procedure. Second, for whole brain perfusions, fixation was accelerated after the initial procedure by injecting fixative into ventricular spaces in the brain using a 50 mL syringe. We employed this additional fixation step to mimic how fixative more readily diffuses into the ventricular system for hemibrains, assuming that the septum pellucidum does not act as a barrier to diffusion, which is expected to be the case following brain hemisection.

Following perfusion, the brains were fixed via additional immersion in 10% (w/v) neutral buffered (sodium phosphate) formalin for approximately two weeks. In the perfusion fixation literature, this subsequent immersion step is referred to as postfixation (McFadden et al., 2019). The two whole brain specimens were imaged with MRI as described below. Then the brains were dissected coronally into slabs 3-5 mm thick in the anterior to posterior direction. Brains were systematically sampled for neuropathologic postmortem diagnosis and placed into cassettes for processing. The samples were embedded in paraffin and 5-7 µm thick sections were cut serially on a microtome, mounted on glass slides, deparaffinized, and stained with hematoxylin and eosin (H&E) or Luxol fast blue counterstained with H&E for microscopic examination. The slides for cases 1, 2, and 3 were viewed and photographed using a Nikon ECLIPSE Ci microscope. The slides for cases 4 and 5 were imaged using a Philips Ultra Fast Scanner.

RNA in situ hybridization

RNA in situ hybridization was performed using the fully automated RNAScope 2.5 LSx Reagent kit-RED (Advanced Cell Diagnostics, catalog #322750) according to the manufacturer's instructions for formalin-fixed paraffin-embedded (FFPE) brain tissue. 5 µm FFPE tissue sections prepared from perfusion fixation brain tissue were baked for 1 hour at 70° C, and the RNAScope assay was run on the Leica BOND Rx automated slide stainer platform (Leica Biosystems). Target retrieval was performed for 20 minutes at 95° C followed by 15 minutes Protease III treatment at 40° C and amplification and detection steps according to the manufactures protocol. A probe for the housekeeping gene ubiquitin C (Hs-UBC, catalog # 312028) was used to assess mRNA detection. Slides were visualized using a Nikon Eclipse brightfield microscope with a Nikon DS-Fi3 camera and NIS Elements software.

Ex vivo whole brain MRI imaging

Following perfusion, both of the two *ex vivo* whole brain specimens were placed in a custom-built imaging container (Boonstra et al., 2021), immersed in Fluorinert (3M, Saint Paul, MN), and exposed to vacuum for 15 minutes to dislodge air bubbles (Stram et al., 2022). The container was sealed, and the specimen was imaged using a 7 Tesla whole-body MRI scanner (Magnetom 7T AS, Siemens, Erlangen, Germany) equipped with a 32-channel radiofrequency head coil (Nova Medical, Wilmington, MA). After acquisition of localizer images and main magnetic field shimming by 3D field mapping, the specimens were imaged with a 3D multi-echo gradient-echo pulse sequence with the following parameters: repetition time = 38 ms, echo times = 5, 10, 15, 20, 25, 30 ms, flip angle = 18°, resolution = 0.38 mm isotropic, in-plane acceleration by GRAPPA (Griswold et al., 2002) with acceleration factor R=2, readout bandwidth = 260 Hz/px, bipolar readouts, non-selective excitation. Individual echo images were co-registered by FSL FLIRT (Jenkinson et al., 2002; Jenkinson and Smith, 2001), and combined into a single image by root-sum-of-squares of individual echoes.

Results

Implementation of the perfusion fixation protocol

We report our deployment of the *ex situ* perfusion fixation procedure on five brains in the form of individual case summaries. In all instances, we used a perfusion circuit with the same core design and evaluated different variations of the procedure. For each case, we describe operational parameters, case-specific factors of the procedure, and metrics recorded regarding the quality of the perfusion fixation for that case (**Table 2**).

Case 1. The perfusion fixation procedure was performed with a hemibrain specimen from a 90+-year-old man with a clinical diagnosis of sepsis who had died of pneumonia. The postmortem interval (PMI) was 52 hours prior to the procedure. Grossly, the blood vessels were assessed as having moderate atherosclerosis. The internal carotid and posterior cerebral arteries were cannulated with a 21G catheter. The vessels were first perfused with 0.5 L of phosphate buffered saline (PBS) with sodium azide (0.01% wt/vol) as a washout solution for 15 minutes. During this washout process, the blood was not found to substantially clear on visual inspection of the surface of the brain. The vessels were next perfused with 1.5 L of fixative solution, consisting of 10% (w/v) formalin and 1% (w/v) glutaraldehyde. Qualitatively, at the end of the fixation procedure, palpation revealed that areas near the perfusate entry were found to be stiffer than other areas of the brain, suggestive of rapid fixation in those areas.

Case 2. This procedure was performed with a hemibrain specimen from a 66-year-old woman with a clinical diagnosis of sepsis who had died of cardiac arrest. The PMI was 44 hours. For most of the PMI, the brain was stored at refrigerator temperature (4° C). The anterior carotid artery and middle cerebral artery were cannulated with 19G catheters. With this specimen, it was more difficult to cannulate the vessels as only partial remnants of the original vessels remained after brain removal. The vessels were first perfused with 0.5 L of washout solution at a pump speed of 50 RPM, consisting of PBS with mannitol (4.5% wt/vol) and sodium nitrite (1% wt/vol). Mannitol was employed to assist with opening of the blood brain barrier, while sodium nitrite was used to assist with vasodilation (Ikeda et al., 2003; Palay et al., 1962). During this washout process, the apparent clearance of blood from some blood vessels was visualized. The vessels were then perfused with about 1 L of fixative, consisting of 10% formalin and 1% glutaraldehyde, at a pump speed of 60 RPM. Physical stiffening of the hemibrain post perfusion was not appreciated, possibly suggesting inadequate perfusion in this case, although we did not use precise measurements of stiffness.

Case 3. The perfusion fixation procedure was performed with a hemibrain specimen from a 77-year-old man with a diagnosis of diffuse Lewy body disease who had died of pneumonia. The PMI was 12 hours. Grossly, the blood vessels were assessed as having mild atherosclerosis. The middle cerebral artery and posterior cerebral artery were cannulated with 19G catheters. To streamline the procedure, washout solution and glutaraldehyde were omitted. The vessels were perfused with 2 L of 10% (w/v) formalin at a pump speed of 60 RPM for 30-40 minutes. At the end of the procedure, the anterolateral aspect of the perfused hemibrain had significant swelling. The reason for the swelling was unclear, but the shorter PMI of the specimen in case 3 may have led to a lower resistance to perfusate flow than in cases 1 and 2, leading to a higher effective perfusion pressure, potentially resulting in blood brain barrier disruption (Schwarzmaier et al., 2022).

Case 4. This perfusion fixation procedure was performed on a whole brain specimen from a 90+-year-old woman who was positive for COVID-19 at the time of death. The PMI was 24 hours. The blood vessels were cannulated with 23G catheters in three different ways. No washout solution was perfused. We first cannulated the bilateral internal carotid arteries and perfused approximately 250 mL of 10% formalin at an initial pump speed of 50 RPM that was subsequently raised to 60 RPM. During this process, it was possible to visualize blood being removed from an artery in the right frontal cortex. The inferior frontal gyrus and inferior temporal gyrus appeared to stiffen. However, there was a concern that the bilateral anterior frontal poles were becoming slightly edematous, although the gross effects of this could not be clearly seen post-perfusion. Additionally, at the beginning of the perfusion, the pressure

Table 2. Operational parameters and outcome metrics of brain perfusion fixation

Parameter	Case 1	Case 2	Case 3	Case 4	Case 5
Age	90+	66	77	90+	64
PMI	52 h	44 h	12 h	24 h	7 h
Fresh whole brain weight	1273 g	1240 g	1070 g	1236 g	1217 g
Specimen type	Hemibrain	Hemibrain	Hemibrain	Whole brain	Whole brain
Vessels cannulated	Internal carotid and posterior cerebral arteries	Anterior carotid and middle cerebral arteries	Middle cerebral and posterior cerebral arteries	Bilateral internal carotid arteries; bilateral anterior communicating arteries; basilar artery*	Bilateral middle cerebral arteries; anterior cerebral artery; vertebral artery*
Washout	PBS with 0.01% (w/v) sodium azide	PBS with 4.5% (w/v) mannitol and 1% (w/v) sodium nitrite	None	None	None
Fixative (volume perfused†)	10% (w/v) formalin and 1% (w/v) glutaraldehyde (1.5 L)	10% (w/v) formalin and 1% (w/v) glutaraldehyde (1 L)	10% formalin (2 L)	10% (w/v) formalin (up to 250 mL per vessel)	10% (w/v) formalin (up to 250 mL per vessel)
Fixative perfusion time	45 min	20 min	30-40 min	5-10 min per vessels cannulated	5-10 min per vessels cannulated
Maximum pump speed‡	40 (RPM)	60 RPM	60 RPM	60 RPM	50 RPM
Maximum pressure recorded	NA§	NA	NA	2.1 PSI (108.6 mmHg)	3 PSI (155.1 mmHg)
Pigmentation change	No substantial blood clearing found	Some blood vessels appeared to be drained of blood during washout	No substantial blood clearing found	Blood was visualized being cleared from individual arteries; grossly, the brain appears paler post-perfusion	Clearing of blood appreciated in proximal areas of tissue next to the cannulated blood vessel
Volume change	No major change observed	No major change observed	The anterolateral aspect of the perfused hemibrain had significant swelling	The bilateral anterior frontal poles appeared to become slightly edematous	No major change observed
Mechanical property change	Areas near perfusate entry were found to be stiffer	The hemibrain was not found to be clearly stiffer	The swollen area of the hemibrain was found to be stiffer	The inferior frontal gyrus and inferior temporal gyrus appeared to become stiffer	There appeared to be stiffening of areas of brain tissue distal to the cannulated vessels
Neuroimaging findings	NA	NA	NA	Parenchymal air bubble artifacts	Parenchymal air bubble artifacts

* Semicolons denote vessels cannulated separately and sequentially.

† Volume perfused approximate.

‡ Flow rate is mediated by pump drive speed. With our circuit, 50 rotations per minute (RPM) corresponds to approximately 38 mL/min and 60 RPM to 50 mL/min.

§ Not available.

monitor was at 1.5 PSI (77.6 mmHg), and it increased to approximately 2.1 PSI (108.6 mmHg), suggestive of a possible blockage or buildup of fluid. As a result, the perfusion through the bilateral internal carotid arteries was stopped.

We next cannulated and perfused two other blood vessels to assess whether the same swelling phenomenon would occur. After dissection to remove the cerebellum, it was possible to visualize the circle of Willis, which was intact. We cannulated and perfused through the anterior cerebral arteries bilaterally at a pump speed of 50 RPM. Arteries in the right hemisphere temporal cortex were visualized being drained of blood. However, there was a concern that the vessels may have become clogged because an unintentional pressure increase was detected in the pressure sensor. We then switched to perfusing through the basilar artery at a pump speed of 50 RPM. After a few minutes of perfusion through the basilar artery, the fixative appeared to be accumulating near the circle of Willis rather than penetrating through the blood vessels into the deeper parts of the brain, so this perfusion was stopped. Leakage from the superior cerebellar arteries, which

are severed upon removal of the cerebellum, may have contributed to the observed accumulation of fixative around the circle of Willis.

For injection of fixative, we suspended the whole brain by tying a string around the circle of Willis and placing the specimen into a container filled with formalin. To access the third ventricle, we directly inserted a syringe through the floor of the third ventricle at the posterior aspect of the tuber cinereum and injected 25 mL of 10% formalin. We then inserted a syringe into the cerebral aqueduct and injected 25 mL of 10% formalin there. The brain was then placed on a rocker at refrigerator temperature for postfixation. The gross anatomic condition of this brain shows that the brain grossly appears more pale, suggestive of less remaining blood in vessels, over the course of the preservation process (**Figure 2**).

Case 5. The perfusion fixation procedure was performed on a whole brain specimen from a 64-year-old woman with a clinical diagnosis of metastatic adenocarcinoma. The PMI was 7 hours. The blood vessels were cannulated with 19G catheters in
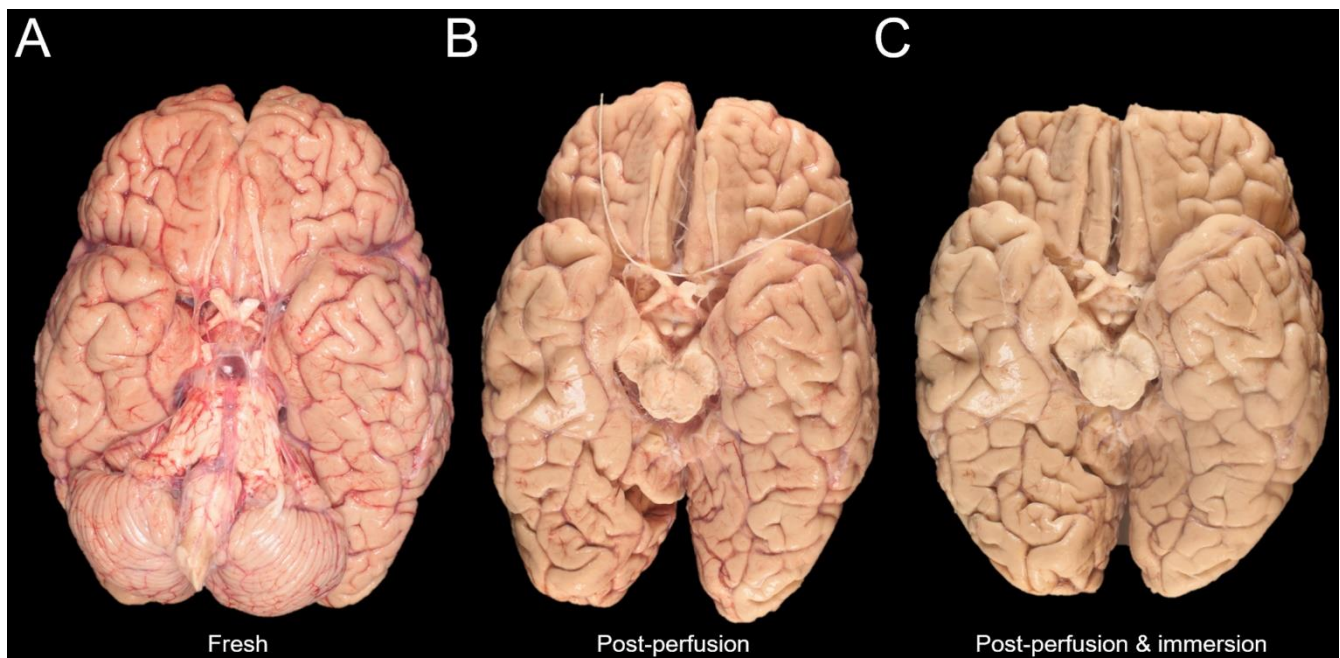

Figure 2. Serial gross images of a donated human brain during *ex-situ* perfusion

The gross anatomic condition of the brain (case 4) is shown via a high-resolution photograph after extraction from the skull but prior to perfusion (**A**), following perfusion fixation and further dissection of the circle of Willis but prior to immersion fixation (**B**), and following both perfusion fixation and post-perfusion immersion fixation (**C**). Note that the cerebellum has been removed from the brain specimen between steps (**A**) and (**B**). Additionally, the frontal pole has been removed at step (**C**).

three different ways. We first cannulated the bilateral middle cerebral arteries, then we cannulated one of the anterior cerebral arteries, and then we cannulated one of the vertebral arteries leading into the basilar artery. After each of these vessel cannulations, we perfused 10% formalin for 5-10 minutes, with no washout solution. The posterior communicating arteries were small and there was no evidence of intact collateral circulation through the circle of Willis.

When perfusing through each of the blood vessels systems in this case, there was clearing of blood appreciated in the proximal areas of the tissue next to the cannulated blood vessel. Manual palpation revealed stiffening of areas of brain tissue distal to the cannulated vessels. The pressure monitoring showed a range of 1.5 PSI (77.6 mmHg) to 2 PSI (103.4 mmHg) when perfusing through two blood vessels. Higher pressures were found, even up to 3 PSI (155.1 mmHg), when perfusing through just one blood vessel. At one point, we also noticed an air bubble to be present in the perfusion tubing, although it is unclear what impact this had on the perfusion quality.
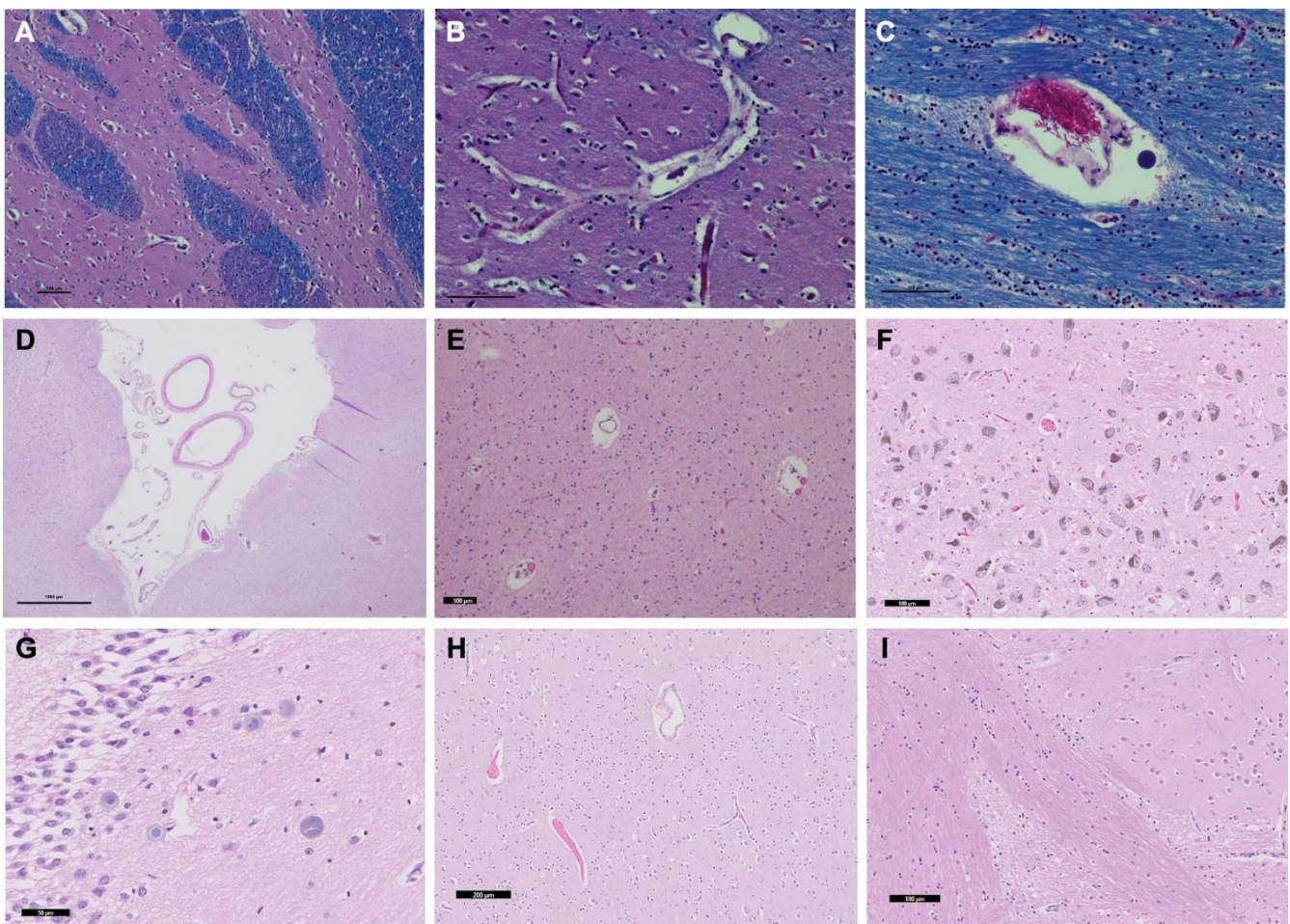

Figure 3. Routinely histology stainings of tissue sections from perfused brains

Representative histology sections were luxol fast blue, hematoxylin and eosin (LH&E)-stained in case 1 (**A-C**) or hematoxylin and eosin (H&E)-stained from case 2 (**D**), case 3 (**E**), case 4 (**F-G**), and case 5 (**H-I**). Sections were derived from the striatum (**A-B**), corpus callosum (**C**), temporal cortex (**D**), white matter of the temporal pole (**E**), substantia nigra (**F**), hippocampus – dentate gyrus (**G**), mid-frontal cortex (**H**), and striatum (**I**). Tissue morphology shows expected findings, suggesting that the perfusion process did not adversely affect tissue morphology. Red blood cells were observed in some vessels, indicating absence of complete perfusion. All scale bars 100 µm except for sub-figures **D** (1000 µm), **G** (50 µm), and **H** (200 µm).

After perfusion, we used a syringe to perform injection fixation of the brain. Fixative was introduced into the third ventricle, the fourth ventricle via a superior approach through the anterior corpus callosum, and each of the lateral ventricles after sectioning through the midbrain and cerebellum. For each injection, we used 25-50 mL of 10% formalin. We infer that the injection was made into the ventricles rather than into the brain parenchyma because a partial flow of fluid could be seen coming out of the perforation in the third ventricle during injection of fixative into the lateral ventricles. Additionally, there was no evidence upon sectioning that the striatum was disrupted, as might have been expected from parenchymal injection. However, because we could not directly visualize the injection into the ventricles, we cannot completely exclude that some of the fixative may have directly entered the brain parenchyma.

Histology and neuroimaging data

Histology data from the perfused brains showed that the expected tissue morphology and cell shape were present, which was similar to typical findings from immersion-fixed brains (**Figure 3**). There were no clear alterations due to the edema observed in the perfused brains.

To assess the distribution of single RNA molecules we performed RNA *in situ* hybridization analysis in one of the perfused brains (**Figure 4**). Specifically, we utilized the RNAScope in situ hybridization (ISH) assay, which is a commercial RNA ISH technology that detects individual mRNA molecules on a single-cell level, in the superior frontal region of case 5 (Wang et al., 2012). We observed a strong and robust ubiquitin C signal in all cell types including neurons, glia and blood vessels, suggesting that mRNA species can be detected in perfused brains (**Figure 4**), as expected from previous results using the RNAscope in immersion-fixed human brain tissue (Baleriola et al., 2014).

We also performed *ex vivo* MRI scans following perfusion of the two whole brains. While pure immersion-based diffusion of formalin has the potential to create an artifact on *ex vivo* MRI scans corresponding to the fixation front, in the MRI scans of perfusion-fixed brains there were no prominent rim artifacts (i.e. variations in signal intensity in superficial versus deep regions) related to inhomogeneous fixation (Nazemorroaya et al., 2022). However, the perfused brains contained numerous small hypointensities seen on multi-echo gradient-echo with root-sum-of-squares echo recombination images, which are not present in comparative immersion-fixed brains scanned with the same protocol (**Figure 5**). These hypointensities are consistent with susceptibility-induced signal loss due to small air bubbles distributed in the vasculature. Therefore, one of the
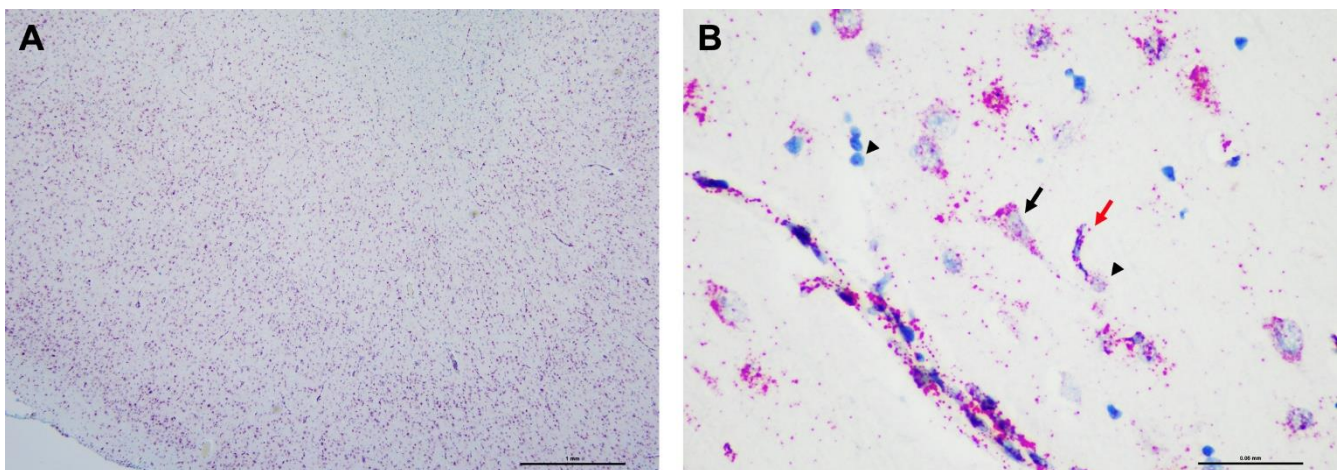

Figure 4. Robust detection of Ubiquitin C RNA by in situ hybridization in a perfusion-fixed brain

Representative low (**A**) and high (**B**) magnification images of the RNAScope assay in the superior frontal region of case five. Strong and robust signal of ubiquitin C mRNA is detected in all cell types including neurons (black arrow), glia (black arrowhead), and blood vessels (red arrow). Scale bars 1 mm (**A**) and 50 μm (**B**).
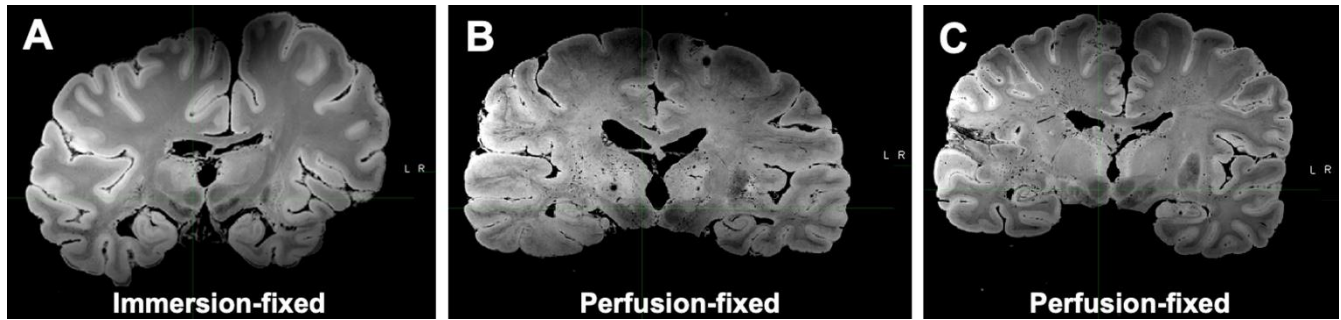
Figure 5. Perfusion-fixed brains contain numerous small hypointensities on MRI scans

Multi-echo gradient-echo with root-sum-of-squares echo recombination images of a comparison immersion-fixed brain (**A**) as well as two perfusion-fixed whole brains: case 4 (**B**) and case 5 (**C**). Numerous small hypointensities are visualized in the two perfusion-fixed brains but not in the immersion-fixed brain imaged with the same protocol.

potential downsides of the current perfusion protocol may be the inadvertent introduction of air bubbles into the tissue. These hypointensities are less likely to be related to perivascular spaces, which typically appear as hyperintensities on these MRI contrasts. However, the effect of these small hypointensities on histological features is uncertain and we have not detected any parenchymal air bubble artifacts in the preliminary histology data reviewed so far.

Discussion

In its simplest form, perfusion fixation can be thought of as an extension of immersion fixation, except that fixative solution extravasates from the blood vessels rather than penetrates from outside brain surfaces. This thereby increases the surface area by which fixatives can penetrate the tissue by orders of magnitude and homogenizes its distribution. However, introducing additional variables causes other potential alterations to the perfused brains that might contribute to artifacts or batch effects in comparison to immersion-fixed brains. Glutaraldehyde, for instance, is not typically used in brain banking and there was a theoretical concern that it might affect the results of downstream immunolabelling assays, introducing the risk of batch effect (Mrini et al., 1995). For this reason, we removed glutaraldehyde from the fixative solution. In further cases, we also removed the washout solution from the protocol. Because formaldehyde takes a significant time to fix tissue, it is unclear if a washout process is necessary to prevent fixation of debris within blood vessels when perfusing with formaldehyde, while using a washout solution adds to procedural complexity and creates a possible batch effect. In our view, the value of perfusing washout solution prior to perfusing fixative remains an open question, with both potential upsides and downsides (McFadden et al., 2019; Tao-Cheng et al., 2007).

A limitation of this technical report is that the recorded outcome metrics were largely qualitative. Because edema was often seen and red blood cells were observed in some vessels, we expect that perfusion fixation was incomplete. However, no quantitative analysis has been performed to determine whether there is a change in autolytic artifacts, blood vessel shape, or other histologic features in the perfused brains compared to brains preserved with the standard immersion protocol (Frigon et al., 2022). As a result, we were unable to quantify the extent of partial perfusion fixation. In future studies, both operational and histologic perfusion fixation quality outcome metrics should be measured more quantitatively. For example, the use of an indentation device that measures both force and displacement could precisely measure tissue stiffness (Elkin et al., 2011). Additionally, the use of video monitoring during the perfusion fixation procedure could help to precisely record and quantify any changes in brain pigmentation or volume. More rigorous outcome metrics would also help to monitor and make any adjustments necessary during the procedure and to optimize the procedure for future cases.

One major challenge in *ex situ* brain perfusion is the presence of air bubbles. Consistent with this,

MRI images from our perfusion-fixed brains showed hypointensities that may correspond to small air bubbles generated or distributed in the vasculature during the perfusion procedure. Because air bubbles will accumulate in sulci, ventricles, and blood vessels as soon as the brain is extracted from the skull, it is an immense challenge to completely avoid air bubbles during *ex situ* perfusion fixation (Bolliger et al., 2018). Air bubbles can also form in the perfusion circuit, which may introduce an unnecessary impediment to perfusion flow. When air bubbles are present in blood vessels, they can theoretically obstruct the flow of fixative. For future iterations of the procedure, we are currently working on a strategy using drip chambers in the perfusion circuit to decrease the potential for air bubbles to be perfused into the blood vessels. Keeping the tubing of the perfusion circle at a vertical angle may also help bubbles to rise to the top rather than continuing through the perfusion circuit.

When a catheter is placed into a blood vessel for cannulation, there is a need to secure it in place, or it will move due to the perfusate flow. Here, we employed hemostats to secure the catheters. With this approach, the length of vessel required for cannulation is limited by the diameter of the hemostat. With the use of our mosquito hemostats, approximately 1 cm of blood vessel is required to adequately secure the cannula. The presence of atherosclerosis did not appear to affect the ability to seal the cannulated vessels. However, hemostats are unwieldy and can obstruct the field of vision. An alternative approach is to use surgical sutures; however, this requires significant skill and takes more time. We are currently evaluating alternative approaches to address the problem of securing catheters in the blood vessels. It is also important to note the necessity of clamping arteries that are downstream of the cannulated artery and that are not wished to be perfused. The failure to clamp severed superior cerebellar arteries may have contributed to the fixative accumulation that occurred during perfusion through the basilar artery in case 4.

The two main methods for driving fluid in perfusion fixation are gravity-based systems and peristaltic pumps. With gravity, a constant pressure is provided with variable flow rate, whereas with a peristaltic pump, a consistent oscillating flow rate is provided irrespective of resistance (Scouten et al., 2006). By monitoring the in-line pressure in our peristaltic pump-based perfusion circuit, we can detect whether there is a build-up of resistance to flow, as indicated by an increase in pressure. For a given cannula size, it is possible to control the pressure by varying the pump speed. Therefore, if a pressure build-up is detected, we can either decrease the pump speed and/or cannulate other arteries (Schwarzmaier et al., 2022; Scouten et al., 2006). Because the perfusion circuit will have a higher resistance when perfusing through one blood vessel as opposed to multiple, lower flow rates may need to be used when perfusing through only one vessel, to avoid raising the perfusion pressure to excessive values, as was seen in case 5.

The ideal pressure value for perfusion fixation, or even the one that best simulates brain-specific physiologic perfusion pressure, is unclear. At lower perfusion pressures, the perfusion may be incomplete and hence fail to sufficiently extravasate into the tissue; while at higher perfusion pressures, the blood brain barrier could be disrupted or blood vessels could rupture (Saliani et al., 2017; Schwarzmaier et al., 2022). Currently, we target an in-line perfusion pressure in the range of 70-100 mm Hg based on theoretical expectations. Further investigation is necessary to query the optimal perfusion pressure for the *ex situ* human brain. We speculate that the tissue swelling that we sometimes detected may have resulted from an overly high perfusion pressure (Schwarzmaier et al., 2022). If tissue swelling is detected, suggesting increased resistance to flow, then an alternative approach may be to decrease the perfusion pressure and to perfuse for a longer period of time.

Related to perfusion pressure is the issue of postmortem interval. The postmortem intervals in our sample varied considerably, from 7 hours to 52 hours, which likely contributed to differences in tissue or blood vessel integrity between cases. We hypothesize that factors contributing to resistance to flow are likely to accumulate in brains that have undergone a more severe agonal state or longer postmortem interval prior to the procedure. In those cases, a higher perfusion pressure may be necessary to achieve sufficient perfusate flow throughout the brain. Determining the optimal perfusion pressure

range in brain banking and identifying ways to modify the perfusion pressure during the procedure are important areas for further research.

In addition to uncertainties regarding perfusion pressure, the duration of perfusion fixation to provide adequate tissue fixation is also unclear. In rodent studies, as few as 5 minutes of perfusion fixation at optimal pressure has been found to be sufficient for proper tissue preservation (Schwarzmaier et al., 2022). In brain banking studies, however, reported times of perfusion fixation have varied widely, from 5 minutes to 2 hours, with 15-30 minutes being a commonly reported time range (McFadden et al., 2019). Because of the potential for inadequate perfusate flow in human brains, methods that allow for precise monitoring during the perfusion procedure, such as ultrasound or MRI, may help investigators to tailor the perfusion time for each brain, albeit at higher cost (Vrselja et al., 2019). Taken together, the amount of time required for adequate perfusion fixation and postfixation in brain banking that preserves tissue morphology while minimizing alterations of antigenicity is an important open research question.

Conclusion

In our standard immersion fixation protocol, the whole brain or hemibrain is immersed in formalin for two to four weeks prior to further sectioning and storage procedures. Based on previous data and biophysical principles, there are theoretical reasons to expect that preservation using the perfusion fixation protocol may yield improved histology quality (McFadden et al., 2019). However, we do not have any systematic outcome data comparing our perfusion procedure to an immersion procedure. We also encountered several challenges in implementing the perfusion fixation procedure, including the intermittent occurrence of tissue swelling and the potential for introducing air bubbles into the vasculature. The added value to preservation quality using a perfusion fixation approach may depend in part on the agonal phase and the postmortem interval, during which thrombi may accumulate and blood vessels undergo autolysis, thereby restricting perfusate flow (Hansma et al., 2015). Further research and development are needed to improve the rigor and reproducibility of perfusion fixation methods and to assess the value of the procedure in improving preservation quality.

Acknowledgements

Abbreviations

PBS: Phosphate buffered saline; PMI: Postmortem interval; MRI: Magnetic resonance imaging; RPM: Rotations per minute.

Author Contributions

A.T.M., K.D.-O.C., A.S., Z.W., E.M.C.H., and J.F.C. contributed to the original conception of the study; A.T.M., E.W.-L., A.C., H.W., and J.F.C. performed perfusion fixation studies; E.W.-L. and D.D. performed histology studies; K.W. performed RNA in situ hybridization studies; A.S. performed MRI imaging and data analysis; A.T.M. and J.F.C. wrote the original draft of the manuscript. All authors read and approved the manuscript.

Conflict of interest

The authors declare that they have no competing financial interests.

Data availability

All histology and MRI data presented is available to the academic community upon request.

References

Adickes, E.D., Folkerth, R.D., Sims, K.L., 1997. Use of perfusion fixation for improved neuropathologic examination. Arch. Pathol. Lab. Med. 121, 1199–1206.

Baleriola, J., Walker, C.A., Jean, Y.Y., Crary, J.F., Troy, C.M., Nagy, P.L., Hengst, U., 2014. Axonally synthesized ATF4 transmits a neurodegenerative signal across brain regions. Cell 158, 1159–1172. https://doi.org/10.1016/j.cell.2014.07.001

Beach, T.G., Tago, H., Nagai, T., Kimura, H., McGeer, P.L., McGeer, E.G., 1987. Perfusion-fixation of the human brain for immunohistochemistry: comparison with immersion-fixation. J. Neurosci. Methods 19, 183–192. https://doi.org/10.1016/s0165-0270(87)80001-8

Bodian, D., 1936. A new method for staining nerve fibers and nerve endings in mounted paraffin sections. Anat. Rec. 65, 89–97. https://doi.org/10.1002/ar.1090650110

Bolliger, S.A., Tomasin, D., Heimer, J., Richter, H., Thali, M.J., Gascho, D., 2018. Rapid and reliable detection of previous freezing of cerebral tissue by computed tomography and magnetic resonance imaging. Forensic Sci. Med. Pathol. 14, 85–94. https://doi.org/10.1007/s12024-018-9955-0

Boonstra, J.T., Michielse, S., Roebroeck, A., Temel, Y., Jahanshahi, A., 2021. Dedicated container for postmortem human brain ultra-high field magnetic resonance imaging. NeuroImage 235, 118010. https://doi.org/10.1016/j.neuroimage.2021.118010

de Oliveira, K.C., Nery, F.G., Ferreti, R.E.L., Lima, M.C., Cappi, C., Machado-Lima, A., Polichiso, L., Carreira, L.L., Ávila, C., Alho, A.T.D.L., Brentani, H.P., Miguel, E.C., Heinsen, H., Jacob-Filho, W., Pasqualucci, C.A., Lafer, B., Grinberg, L.T., 2012. Brazilian psychiatric brain bank: a new contribution tool to network studies. Cell Tissue Bank. 13, 315–326. https://doi.org/10.1007/s10561-011-9258-0

Elkin, B.S., Ilankova, A., Morrison, B., 2011. Dynamic, regional mechanical properties of the porcine brain: indentation in the coronal plane. J. Biomech. Eng. 133, 071009. https://doi.org/10.1115/1.4004494

Frigon, È.-M., Dadar, M., Boire, D., Maranzano, J., 2022. Antigenicity is preserved with fixative solutions used in human gross anatomy: A mice brain immunohistochemistry study. https://doi.org/10.1101/2022.05.06.490908

Grinberg, L.T., Amaro, E., Teipel, S., dos Santos, D.D., Pasqualucci, C.A., Leite, R.E.P., Camargo, C.R., Gonçalves, J.A., Sanches, A.G., Santana, M., Ferretti, R.E.L., Jacob-Filho, W., Nitrini, R., Heinsen, H., Brazilian Aging Brain Study Group, 2008. Assessment of factors that confound MRI and neuropathological correlation of human postmortem brain tissue. Cell Tissue Bank. 9, 195–203. https://doi.org/10.1007/s10561-008-9080-5

Griswold, M.A., Jakob, P.M., Heidemann, R.M., Nittka, M., Jellus, V., Wang, J., Kiefer, B., Haase, A., 2002. Generalized autocalibrating partially parallel acquisitions (GRAPPA). Magn. Reson. Med. 47, 1202–1210. https://doi.org/10.1002/mrm.10171

Halliday, G.M., Li, Y.W., Joh, T.H., Cotton, R.G., Howe, P.R., Geffen, L.B., Blessing, W.W., 1988. Distribution of substance P-like immunoreactive neurons in the human medulla oblongata: co-localization with monoamine-synthesizing neurons. Synapse 2, 353–370. https://doi.org/10.1002/syn.890020403

Hansma, P., Powers, S., Diaz, F., Li, W., 2015. Agonal thrombi at autopsy. Am. J. Forensic Med. Pathol. 36, 141–144. https://doi.org/10.1097/PAF.0000000000000162

Ikeda, M., Nagashima, T., Bhattacharjee, A.K., Kondoh, T., Kohmura, E., Tamaki, N., 2003. Quantitative analysis of hyperosmotic and hypothermic blood-brain barrier opening. Acta Neurochir. Suppl. 86, 559–563. https://doi.org/10.1007/978-3-7091-0651-8_114

Insausti, R., Tuñón, T., Sobreviela, T., Insausti, A.M., Gonzalo, L.M., 1995. The human entorhinal cortex: a cytoarchitectonic analysis. J. Comp. Neurol. 355, 171–198. https://doi.org/10.1002/cne.903550203

Jenkinson, M., Bannister, P., Brady, M., Smith, S., 2002. Improved optimization for the robust and accurate linear registration and motion correction of brain images. NeuroImage 17, 825–841. https://doi.org/10.1016/s1053-8119(02)91132-8

Jenkinson, M., Smith, S., 2001. A global optimisation method for robust affine registration of brain images. Med. Image Anal. 5, 143–156. https://doi.org/10.1016/s1361-8415(01)00036-6

Karlsson, U., Schultz, R.L., 1965. Fixation of the Central Nervous System for Electron Microscopy by Aldehyde Perfusion. 1. Preservation with Aldehyde Perfusates versus Direct Perfusion with Osmium Tetroxide with Special Reference to Membranes and the Extracellular Space. J. Ultrastruct. Res. 12, 160–186. https://doi.org/10.1016/s0022-5320(65)80014-4

Lucassen, P.J., Chung, W.C., Kamphorst, W., Swaab, D.F., 1997. DNA damage distribution in the human brain as shown by in situ end labeling; area-specific differences in aging and Alzheimer disease in the absence of apoptotic morphology. J. Neuropathol. Exp. Neurol. https://doi.org/10.1097/00005072-199708000-00007

Manger, P.R., Pillay, P., Maseko, B.C., Bhagwandin, A., Gravett, N., Moon, D.-J., Jillani, N., Hemingway, J., 2009. Acquisition of brains from the African elephant (Loxodonta africana): perfusion-fixation and dissection. J. Neurosci. Methods 179, 16–21. https://doi.org/10.1016/j.jneumeth.2009.01.001

McFadden, W.C., Walsh, H., Richter, F., Soudant, C., Bryce, C.H., Hof, P.R., Fowkes, M., Crary, J.F., McKenzie, A.T., 2019. Perfusion fixation in brain banking: a systematic review. Acta Neuropathol. Commun. 7, 146. https://doi.org/10.1186/s40478-019-0799-y

Mrini, A., Moukhles, H., Jacomy, H., Bosler, O., Doucet, G., 1995. Efficient immunodetection of various protein antigens in glutaraldehyde-fixed brain tissue. J. Histochem. Cytochem. Off. J. Histochem. Soc. 43, 1285–1291. https://doi.org/10.1177/43.12.8537644

Musigazi, G.U., De Vleeschauwer, S., Sciot, R., Verbeken, E., Depreitere, B., 2018. Brain perfusion fixation in male pigs using a safer closed system. Lab. Anim. 52, 413–417. https://doi.org/10.1177/0023677217752747

Nazemorroaya, A., Aghaeifar, A., Shiozawa, T., Hirt, B., Schulz, H., Scheffler, K., Hagberg, G.E., 2022. Developing formalin-based fixative agents for post mortem brain MRI at 9.4 T. Magn. Reson. Med. 87, 2481–2494. https://doi.org/10.1002/mrm.29122

Palay, S.L., McGee-Russell, S.M., Gordon, S., Grillo, M.A., 1962. Fixation of neural tissues for electron microscopy by perfusion with solutions of osmium tetroxide. J. Cell Biol. 12, 385–410. https://doi.org/10.1083/jcb.12.2.385

Pallebage-Gamarallage, M., Foxley, S., Menke, R.A.L., Huszar, I.N., Jenkinson, M., Tendler, B.C., Wang, C., Jbabdi, S., Turner, M.R., Miller, K.L., Ansorge, O., 2018. Dissecting the pathobiology of altered MRI signal in amyotrophic lateral sclerosis: A post mortem whole brain sampling strategy for the integration of ultra-high-field MRI and quantitative neuropathology. BMC Neurosci. 19, 11. https://doi.org/10.1186/s12868-018-0416-1

Patel, K.B., Liang, W., Casper, M.J., Voleti, V., Li, W., Yagielski, A.J., Zhao, H.T., Perez Campos, C., Lee, G.S., Liu, J.M., Philipone, E., Yoon, A.J., Olive, K.P., Coley, S.M., Hillman, E.M.C., 2022. High-speed light-sheet microscopy for the in-situ acquisition of volumetric histological images of living tissue. Nat. Biomed. Eng. 6, 569–583. https://doi.org/10.1038/s41551-022-00849-7

Saliani, A., Perraud, B., Duval, T., Stikov, N., Rossignol, S., Cohen-Adad, J., 2017. Axon and myelin morphology in animal and human spinal cord. Front. Neuroanat. 11. https://doi.org/10.3389/fnana.2017.00129

Schwarzmaier, S.M., Knarr, M.R.O., Hu, S., Ertürk, A., Hellal, F., Plesnila, N., 2022. Perfusion pressure determines vascular integrity and histomorphological quality following perfusion fixation of the brain. J. Neurosci. Methods 372, 109493. https://doi.org/10.1016/j.jneumeth.2022.109493

Scouten, C.W., O'Connor, R., Cunningham, M., 2006. Perfusion fixation of research animals. Microsc. Today 14, 26–33. https://doi.org/10.1017/S1551929500057631

Shapson-Coe, A., Januszewski, M., Berger, D.R., Pope, A., Wu, Y., Blakely, T., Schalek, R.L., Li, P.H., Wang, S., Maitin-Shepard, J., Karlupia, N., Dorkenwald, S., Sjostedt, E., Leavitt, L., Lee, D., Bailey, L., Fitzmaurice, A., Kar, R., Field, B., Wu, H., Wagner-Carena, J., Aley, D., Lau, J., Lin, Z., Wei, D., Pfister, H., Peleg, A., Jain, V., Lichtman, J.W., 2021. A connectomic study of a petascale fragment of human cerebral cortex. https://doi.org/10.1101/2021.05.29.446289

Stram, M.N., Seifert, A.C., Cortes, E., Akyatan, A., Woodoff-Leith, E., Borukhov, V., Tetlow, A., Alyemni, D., Greenberg, M., Gupta, A., Krausert, A., Mecca, L., Rodriguez, S., Stahl-Herz, J., Guzman, M.A., Delman, B., Crary, J.F., Dams-O'Connor, K., Folkerth, R.D., 2022. Neuropathology of Pediatric SARS-CoV-2 Infection in the Forensic Setting: Novel Application of Ex Vivo Imaging in Analysis of Brain Microvasculature. Front. Neurol. 13, 894565. https://doi.org/10.3389/fneur.2022.894565

Tao-Cheng, J.-H., Gallant, P.E., Brightman, M.W., Dosemeci, A., Reese, T.S., 2007. Structural changes at synapses after delayed perfusion fixation in different regions of the mouse brain. J. Comp. Neurol. 501, 731–740. https://doi.org/10.1002/cne.21276

Vrselja, Z., Daniele, S.G., Silbereis, J., Talpo, F., Morozov, Y.M., Sousa, A.M.M., Tanaka, B.S., Skarica, M., Pletikos, M., Kaur, N., Zhuang, Z.W., Liu, Z., Alkawadri, R., Sinusas, A.J., Latham, S.R., Waxman, S.G., Sestan, N., 2019. Restoration of brain circulation and cellular functions hours post-mortem. Nature 568, 336–343. https://doi.org/10.1038/s41586-019-1099-1

Waldvogel, H.J., Curtis, M.A., Baer, K., Rees, M.I., Faull, R.L.M., 2006. Immunohistochemical staining of post-mortem adult human brain sections. Nat. Protoc. 1, 2719–2732. https://doi.org/10.1038/nprot.2006.354

Wang, F., Flanagan, J., Su, N., Wang, L.-C., Bui, S., Nielson, A., Wu, X., Vo, H.-T., Ma, X.-J., Luo, Y., 2012. RNAscope: a novel in situ RNA analysis platform for formalin-fixed, paraffin-embedded tissues. J. Mol. Diagn. JMD 14, 22–29. https://doi.org/10.1016/j.jmoldx.2011.08.002

Welikovitch, L.A., Do Carmo, S., Maglóczky, Z., Szocsics, P., Lőke, J., Freund, T., Cuello, A.C., 2018. Evidence of intraneuronal Aβ accumulation preceding tau pathology in the entorhinal cortex. Acta Neuropathol. (Berl.) 136, 901–917. https://doi.org/10.1007/s00401-018-1922-z